

Analyst

Accepted Manuscript



This is an *Accepted Manuscript*, which has been through the Royal Society of Chemistry peer review process and has been accepted for publication.

Accepted Manuscripts are published online shortly after acceptance, before technical editing, formatting and proof reading. Using this free service, authors can make their results available to the community, in citable form, before we publish the edited article. We will replace this *Accepted Manuscript* with the edited and formatted *Advance Article* as soon as it is available.

You can find more information about *Accepted Manuscripts* in the [Information for Authors](#).

Please note that technical editing may introduce minor changes to the text and/or graphics, which may alter content. The journal's standard [Terms & Conditions](#) and the [Ethical guidelines](#) still apply. In no event shall the Royal Society of Chemistry be held responsible for any errors or omissions in this *Accepted Manuscript* or any consequences arising from the use of any information it contains.

1
2
3
4
5 Nanoparticle-assisted laser desorption/ionization using sinapic acid-modified iron
6 oxide-nanoparticles for mass spectrometry analysis
7
8

9
10 Hanaka KOMORI[†], Riho HASHIZAKI[†], Issey OSAKA[‡], Takao HIBI[†], Hajime
11 KATANO[†], and Shu TAIRA^{†*}
12
13

14
15
16
17 [†] Department of Bioscience, Fukui Prefectural University, Eiheiji, Fukui 910-1195,
18 Japan
19

20
21 [‡] Center for Nano Materials and Technology, Advanced Institute of Science and
22 Technology, 1-1 Asahidai, Nomi-shi, Ishikawa 923-1292, Japan
23
24

25
26 *Corresponding author: staira@fpu.ac.jp
27
28
29
30
31
32
33
34
35
36
37
38
39
40
41
42
43
44
45
46
47
48
49
50
51
52
53
54
55
56
57
58
59
60

Abstract

Iron oxide-based nanoparticles (NP) were covalently modified with sinapic acid (SA) through a condensation reaction to assist the ionization of both large and small molecules. The morphology of SA-modified-NPs (SA-NP) was characterized by transmission electron microscopy (TEM), and the modification of the NP surface with SA was confirmed with ultraviolet (UV) and infrared (IR) spectroscopy. The number of SA was estimated to be 6 per NP. SA-NP-assisted laser desorption/ionization was carried out on small molecules, such as pesticides and plant hormone, and large molecules, such as peptides and proteins. Peptide fragment from degraded proteins was detected more efficiently compared with conventional methods.

Introduction

Mass spectrometry (MS) is a powerful tool for the analysis of many target molecules. However, it must be coupled with other ionization methods such as secondary ion MS (SIMS) or electrospray ionization (ESI) for the analysis of small molecules, or with matrix-assisted laser desorption/ionization (MALDI) for the analysis of large molecules. The MALDI MS technique is used for the analysis of large molecules such as proteins,¹ nucleic acids,² and synthetic polymers.³ However, MALDI is not suitable for the analysis of small molecules due to ionization of the organic matrices, which produces noise in the low molecular weight region of the mass spectra.

As other ionization assisting material, nanomaterials were used. The role of NPs playing in desorption/ionization of the analytes was considered that metal oxide based-NP has absorption of UV and occurred rapid heating. This thermal energy enhanced desorption from solid phase to gas phase and involved ionization, continuously. In addition, high melt and boiling point of metal oxide based-NP hardly ionize itself that reduce background at small m/z region. In the first demonstration of nanomaterial-based ionization MS, a mixture of cobalt-oxide nanoparticles and glycerol was used to ionize proteins⁴, although ionization efficiency of analyte was lower than that of organic matrices. Thus nanomaterial-based ionization was not major in the LDI method. Recently, nanomaterial-based ionization method attracted MS field's attention for ionization of small molecules producing a large background signal in the low mass region ($<m/z$ 500). Noble metal-based nanoflowers were used to induce the ionization of target samples, resulting in high-resolution signals.^{5, 6} We have also developed nanoparticle-assisted laser desorption/ionization mass spectrometry (nano-PALDI MS) has been used to ionize both small and large molecules without background signal in the low mass region. The metal oxide core of the particles absorbs the laser radiation, and the silicate network and amino group covering the particles transfer some of the energy to the analyte. Additionally, the ionization of pesticides,⁷ peptides,⁸ and oligonucleotides⁹ has been demonstrated using nano-PALDI MS. The ionization of insulin (Mw: 5,803) has also been demonstrated at a maximum using iron-oxide core-based nanoparticles.¹⁰ Previous reports described conjugation of chemical matrices on NP's surface^{11, 12}. These have drastically improved the ionization efficiency target molecule without chemical noises, although these targets were not high molecules. If nano-PALDI can be used to efficiently ionize small and large molecules, additional

1
2
3
4
5
6
7
8
9
10
11
12
13
14
15
16
17
18
19
20
21
22
23
24
25
26
27
28
29
30
31
32
33
34
35
36
37
38
39
40
41
42
43
44
45
46
47
48
49
50
51
52
53
54
55
56
57
58
59
60

ionization methods are not needed.

The present study describes the synthesis of new functionalized iron-oxide NP as a replacement for conventional chemical matrices to promote the ionization of small and large molecules such as pesticides, plant hormone, peptides, and proteins. Sinapic acid (SA) has been used as a matrix in MALDI of various large molecules. Here, the carboxy group of SA was covalently bonded to an amino group on the iron oxide-based NP surface via condensation (Figure 1). The physical characteristics of the SA-modified NPs (SA-NP) were determined and their ability to ionize both small and large molecules using SA-NP-based nano-PALDI MS was evaluated.

Experimental

Preparation of iron oxide-based nanoparticles (NP)

The NPs were prepared by adding an aqueous solution of $\text{FeCl}_2 \cdot 4\text{H}_2\text{O}$ (0.1 M; 20 mL) (Wako Pure Chemicals, Japan) to 20 mL of γ -aminopropyltriethoxysilane (γ -APTES) (Shin-Etsu Chemicals, Japan). After stirring for 1 h at room temperature, the solution was centrifuged at 15 krpm (Hitachi, CF15RXII) at 4 °C for 1 h. The resulting precipitate was washed three times with ultrapure water. Finally, the precipitate was suspended in *N,N*-dimethylformamide (DMF).

Synthesis of organic matrix-modified NPs (SA-NP)

Sinapic acid (SA) or α -cyano-4-hydroxycinnamic acid (CHCA) or 2,5-dihydroxybenzoic acid (DHB) (0.1 M) and carbonyldiimidazole (CDI; 0.2 M) were dissolved in DMF (5 mL), respectively. This solution was added to a NP suspension (5 mL) and heated to 35 °C. After stirring for 20 h, the solution was centrifuged at 15 krpm for 4 °C for 1 h. The resulting precipitate was washed three times with DMF, suspended in MeOH, and stored at 4 °C.

Characterization of the SA-NPs

Optical absorption spectra of the SA-NPs were recorded using a UV spectrometer (Jasco, V-630, Japan). The presence of SA on the NPs was confirmed with a Fourier-transform infrared spectrometer (FT-IR; Perkin Elmer; Spectrum Two, USA). The morphology and size distribution of the SA-NPs were investigated with a transmission electron microscope (TEM; Hitachi, H-7650, Japan).

Nano-PALDI MS

The usefulness of SA-NPs as an ionization-assisting material in mass spectrometry was investigated using a MALDI time-of-flight (TOF) instrument (Bruker; Autoflex) equipped with a nitrogen laser emitting at 337 nm. Carbendazim (Mw: 191), abscisic acid (ABA, Mw: 264), angiotensin II (Mw: 1,045), Amyloid-beta (A β , Mw: 4,329), insulin (Mw: 5,803), and cytochrome C (Mw: 12,360) were used as examples of both small and large molecules (final sample concentration of 10 pmol/ μ L). Suspensions containing one of the above samples and SA-NPs (1 mg/mL) were dropped onto a target plate using a pipette. The analyte surface was irradiated with 1,000 laser shots and TOF spectra were acquired in positive ion detection mode. To measure the degradation of proteins, a degraded insulin sample was prepared using trypsin. Dithiothreitol (DTT) (1 M, 1 μ L) was added to a solution of insulin (0.5 mg/mL) in ammonium bicarbonate buffer and the mixture was incubated for 1 hour at 37 $^{\circ}$ C. After cleavage of the insulin disulfide bonds, the solution was diluted with ammonium bicarbonate buffer (400 μ L) and more trypsin was added (final concentration of 10 μ g/mL) to digest the insulin. After incubation for 4 hours at 37 $^{\circ}$ C, the sample was analyzed by nano-PALDI and MALDI MS to a short fragment sequence (GFFYTPK; Mw: 859.4)¹³.

Results and discussion

The SA-NPs were analyzed by FT-IR to confirm chemical bonding between the SA molecules and the surface of the NPs. The spectrum of the original NPs contained signals for the N-H and C-N bonds of γ -APTES at 1,550-1,640 and 1,455 cm^{-1} , respectively (Fig. 2A-i). For the SA-NPs, the signal for the aromatic ring of SA was observed at 1,625-1,475 cm^{-1} and the amide bond between the carboxy group of SA and the amino group of APTES on the NPs was observed at 1,650 (C=O stretch) and 1,540 and 1,240 cm^{-1} (N-H stretch) (Fig. 2A-ii). The NP spectrum contained no absorption at 200-500 nm (Fig. 2B-i). The UV absorption spectrum of SA contained signals at 220 and 350 nm corresponding to the carboxy and benzyl groups, respectively (Fig. 2B-ii), while the spectrum of the SA-NPs showed an absorption at 340 nm. This is due to the change in electron state of the benzyl group, and amide bond between the carboxy group of SA and amino group of NP. The absorption at 220 nm was greater than that of SA due to the disappearance of the carboxy group and the formed amide bond (Fig. 2B-iii); the absorbance index of the amide bond was much greater than that of the

1
2
3
4
5
6
7
8
9
10
11
12
13
14
15
16
17
18
19
20
21
22
23
24
25
26
27
28
29
30
31
32
33
34
35
36
37
38
39
40
41
42
43
44
45
46
47
48
49
50
51
52
53
54
55
56
57
58
59
60

carboxy group. We estimated the amount of SA, DHB and CHCA on NPs to be 5, 10 and 4 $\mu\text{g}/\text{mg-NP}$ by UV-Vis measurement, respectively (supporting information table S1). The mass of the NP is $9.5 \times 10^{-21} \text{ mg}^{14}$. Thus, the number of NP was estimated to be $1 \times 10^{20}/\text{mg}$. In addition, from the FT-IR calibration, we determined the number of amino groups per weight is calculated to be $18 \times 10^{20}/\text{mg}$. Hence, six SAs were modified with a particle. SA density on target plate was $15 \text{ ng}/\text{mm}^2$. Figure 2C shows a TEM image of the SA-NPs. The original NPs had small diameters for both the primary ($3.0 \pm 0.6 \text{ nm}$) and aggregated groups ($n=100$ measurements). The average diameter of the SA-NPs was $2.9 \pm 0.8 \text{ nm}$ ($n=100$ measurements). Therefore, no significant difference in size was observed between the original NPs and the SA-NPs. Based on the spectroscopic and TEM results, modification of SA on the NP surface and morphology was confirmed.

To verify the ionization ability of SA-NP, carbendazim, ABA, angiotensin II, $\text{A}\beta$, insulin, and cytochrome C were analyzed using MS under MALDI conditions. The SA-NPs were used to ionize insulin (Fig. 3A-i), resulting in a 28-fold increase in the ionization intensity compared with that provided by the original NPs (Fig. 3A-ii). The saturated SA had 1.6-fold greater intensity than that of the SA-NPs (Fig. 3A-iii). However, at same density of SA condition, SA-NP showed 4.0-fold greater intensity than that of the SA (Fig. 3A-iv), indicating that the ionization efficiency of large molecule depends the amount of SA. Thus, the use of saturated SA as an organic matrix more strongly promotes the ionization of large molecules than SA-NP. However, SA-NP could be used to detect the small molecule carbendazim and ABA without noise (Fig. 3B-i), while SA produced background noise due to self-ionization (Fig. 3B-ii). Protein degradation was also examined. After digestion of insulin by trypsin, the fragment sequence GFFTYPK (Mw: 859) was produced. Figure 3C-i shows the MS spectra of the degraded insulin sample. The nano-PALDI MS spectrum contained protonated fragment sequences, which can only be detected marginally by the MALDI method. The ionization ratio was 200:1. Because the SA predominantly ionized itself (Fig. 3C-ii), the fragment sequence was affected by ionization suppression. At same density of matrix on target plate, as control experiment, SA-NP could ionize proteins at 60 (J) of laser power, but DHB- and CHCA-NP hardly ionize it. DHB- and CHCA-NP could ionize fragment of protein at higher energy condition 11 (J) (supporting information figure S2). Thus, SA-NP was more useful than SA for small to large target molecules.

1
2
3
4
5
6
7
8
9
10
11
12
13
14
15
16
17
18
19
20
21
22
23
24
25
26
27
28
29
30
31
32
33
34
35
36
37
38
39
40
41
42
43
44
45
46
47
48
49
50
51
52
53
54
55
56
57
58
59
60

Angiotensin II, A β , and cytochrome C were also tested. The original NPs could ionize angiotensin II and A β , which produced fragments in the medium m/z range, although they could not ionize the large molecule cytochrome C. However, the SA-NPs could ionize samples larger than 10 kDa (Fig. 4). Normally, we should choose ionization methods and instruments by molecular weight of analyte. Thus, SA-NPs are more useful for ionization across a wide range of molecular weights using a single ionization method id est nano-PALDI method.

Conclusions

The surface of metal oxide NPs could be modified through covalent bonding to amino groups on SA. Because the SA-modified-NPs did not undergo self-ionization, no background noise was produced (unlike SA only, which produced a noise signal in the low molecular weight region). The SA-NPs acted as an ionization-assisting reagent for both small and large molecules. SA-NP-based nano-PALDI can be used to analyze molecules of a wide range of molecular weights. This method represents an advancement in various areas of applied industrial chemistry, such as for the use of polymers and additives on electronic substrates and for mass spectrometry imaging.

Acknowledgements

We thank members of the Katano and Hibi Laboratories in FPU for providing technical assistance and advice. This research was supported by a Lotte grant, Cosmetology foundation grant and a SUNBOR grant to S.T.

References

1. K. R. Reiding, D. Blank, D. M. Kuijper, A. M. Deelder and M. Wührer, *Anal. Chem.*, 2014, **86**, 5784-5793.
2. I. Garaguso, R. Halter, J. Krzeminski, S. Amin and J. Borlak, *Anal. Chem.*, 2010, **82**, 8573-8582.
3. K. Krueger, C. Terne, C. Werner, U. Freudenberg, V. Jankowski, W. Zidek and J. Jankowski, *Anal. Chem.*, 2013, **85**, 4998-5004.
4. K. Tanaka, Y. Ido, S. Akita, Y. Yoshida and T. Yoshida, *Proceedings of the 2nd Japan-China Joint Symposium on Mass spectrometry*, 1987, 185-187.

- 1
 - 2
 - 3
 - 4
 - 5
 - 6
 - 7
 - 8
 - 9
 - 10
 - 11
 - 12
 - 13
 - 14
 - 15
 - 16
 - 17
 - 18
 - 19
 - 20
 - 21
 - 22
 - 23
 - 24
 - 25
 - 26
 - 27
 - 28
 - 29
 - 30
 - 31
 - 32
 - 33
 - 34
 - 35
 - 36
 - 37
 - 38
 - 39
 - 40
 - 41
 - 42
 - 43
 - 44
 - 45
 - 46
 - 47
 - 48
 - 49
 - 50
 - 51
 - 52
 - 53
 - 54
 - 55
 - 56
 - 57
 - 58
 - 59
 - 60
5. H. Kawasaki, T. Yonezawa, T. Watanabe and R. Arakawa, *J. Phys. Chem. C* 2007, **111**, 16278-16283.
6. I. Ocsoy, B. Gulbakan, M. I. Shukoor, X. Xiong, T. Chen, D. H. Powell and W. Tan, *ACS Nano*, 2013, **7**, 417-427.
7. S. Taira, M. Tokai, D. Kaneko, H. Katano and Y. Kawamura-Konishi, *J. Agric. Food. Chem.*, 2015, **63**, 6109-6112.
8. S. Taira, K. Kitajima, H. Katayanahi, E. Ichiishi and Y. Ichiyanagi, *Sci. Technol. Adv. Mater.*, 2009, **10**, 034602.
9. S. Taira, I. Osaka, S. Shimma, D. Kaneko, T. Hiroki, Y. Kawamura-Konishi and Y. Ichiyanagi, *Analyst*, 2012, **137**, 2006-2010.
10. S. Taira, Y. Sugiura, S. Moritake, S. Shimma, Y. Ichiyanagi and M. Setou, *Anal. Chem.*, 2008, **80**, 4761-4766.
11. M.-C. Tseng, R. Obena, Y.-W. Lu, P.-C. Lin, P.-Y. Lin, Y.-S. Yen, J.-T. Lin, L.-D. Huang, K.-L. Lu, L.-L. Lai, C.-C. Lin and Y.-J. Chen, *J. Am. Soc. Mass Spectrom.*, 2010, **21**, 1930-1939.
12. J. Duan, M. J. Linman, C. Y. Chen and Q. J. Cheng, *J. Am. Soc. Mass Spectrom.*, 2009, **20**, 1530-1539.
13. H. Liu, Y. Zhang, J. Wang, D. Wang, C. Zhou, Y. Cai and X. Qian, *Anal. Chem.*, 2006, **78**, 6614-6621.
14. S. Moritake, S. Taira, Y. Ichiyanagi, N. Morone, S.-Y. Song, T. Hatanaka, S. Yuasa and M. Setou, *J. Nanosci. Nanotechnol.*, 2007, **7**, 937-944.

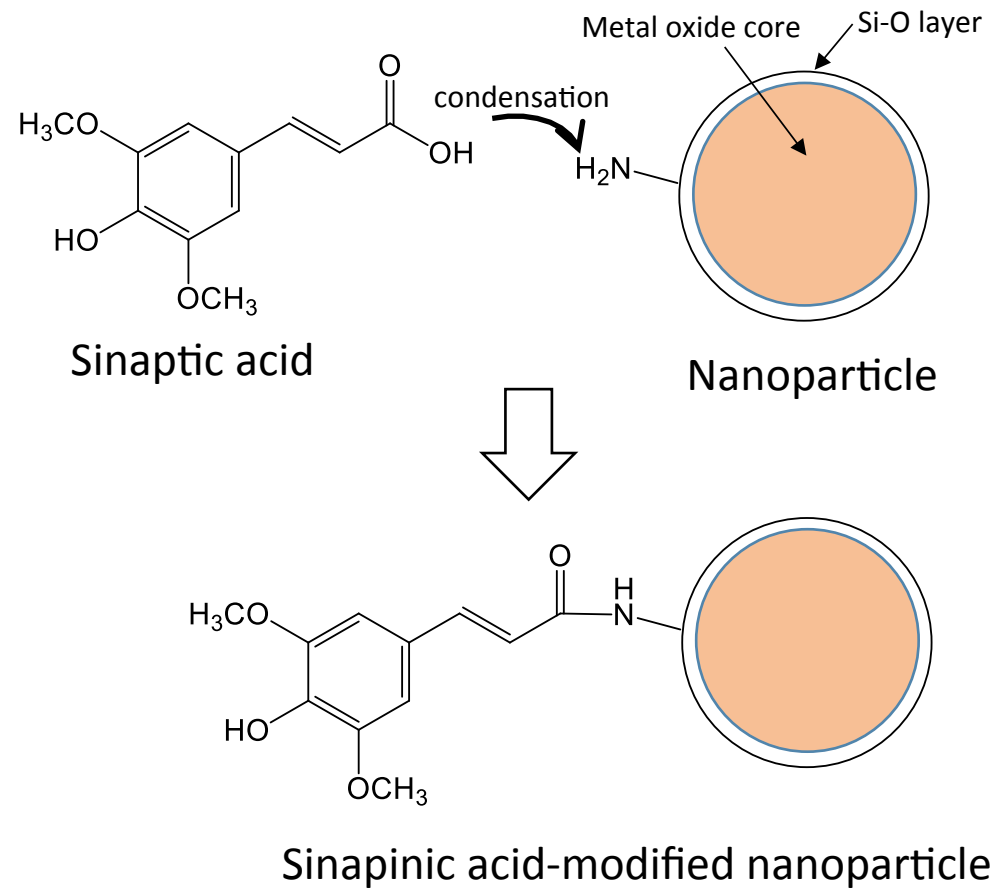


Figure 1 Schematic illustration of synthesis of sinapinic acid-modified nanoparticle

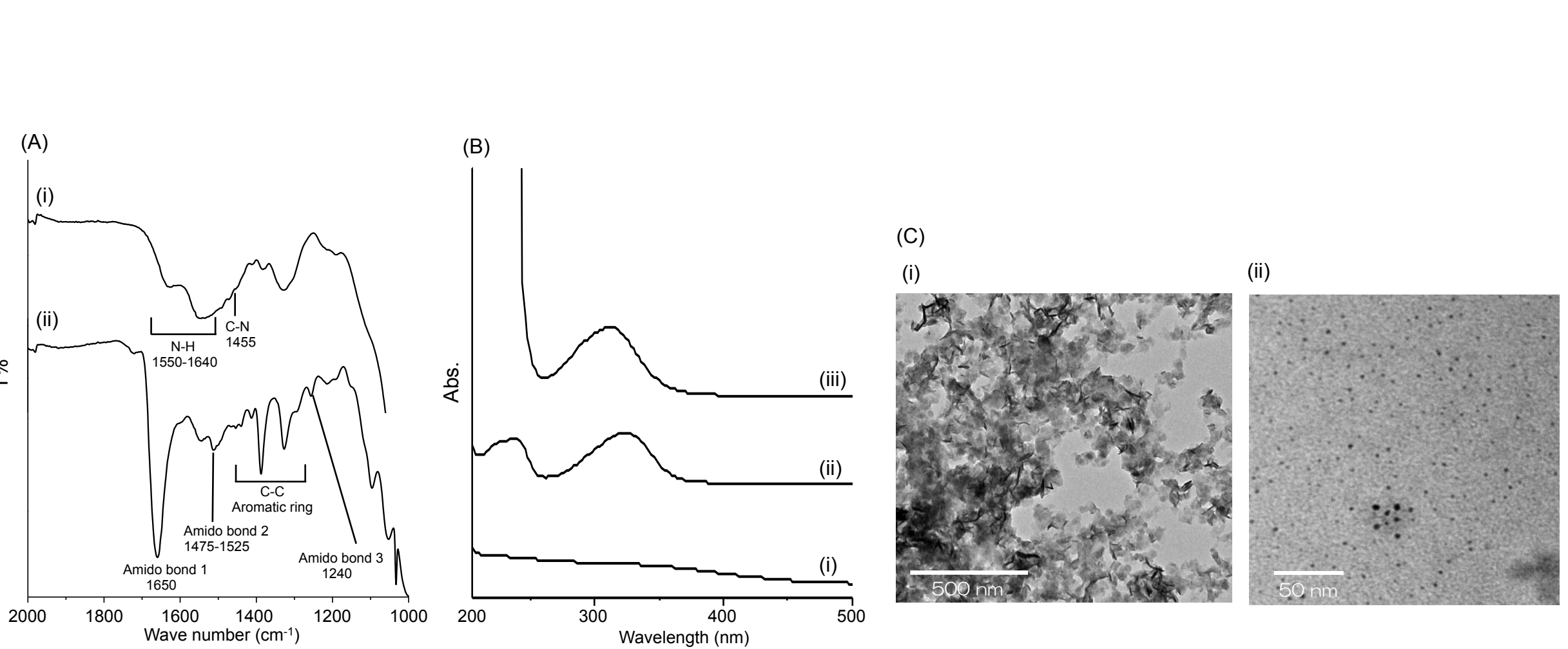


Figure 2 FT-IR spectra of original NP (A-i) and SA-NP (A-ii), absorption spectra of original NP (B-i), SA (B-ii) and SA-NP (B-iii) and, TEM image of SA-NP (magnification for x10 (C-i) and x50 (C-ii))

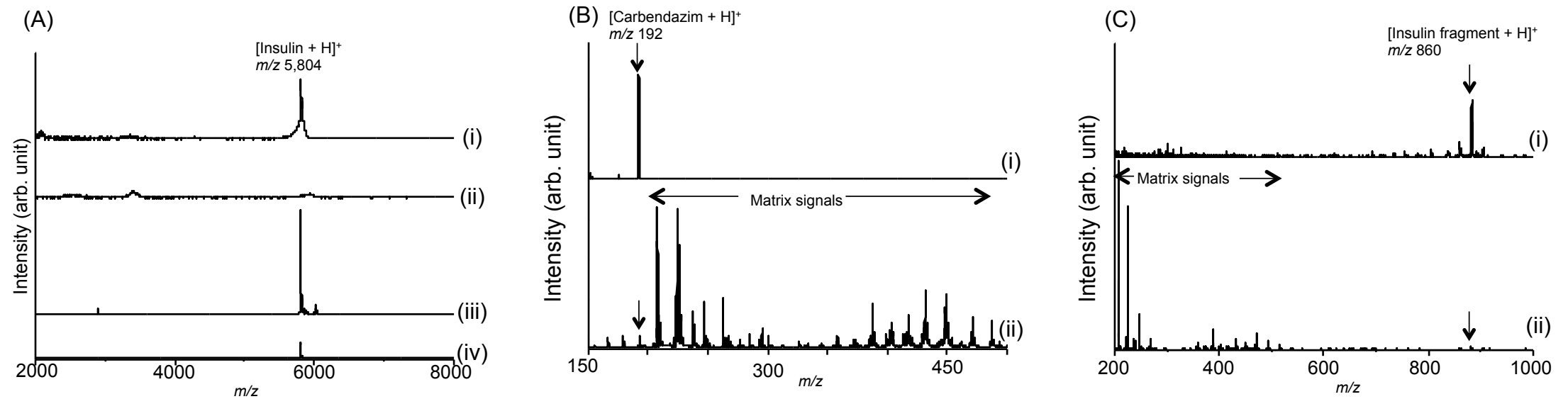


Figure 3. MS spectra of insulin ionized by (A-i) SA-NP, (A-ii) original NP, (A-iii) saturated SA and SA which is prepared to same density of SA of SA-NP (A-iv). MS spectra of carbendazim and ABA ionized by (B-i) SA-NP and (B-ii) SA, and of the insulin fragment GFFYTPK ionized by (C-i) SA-NP and (C-ii) SA.

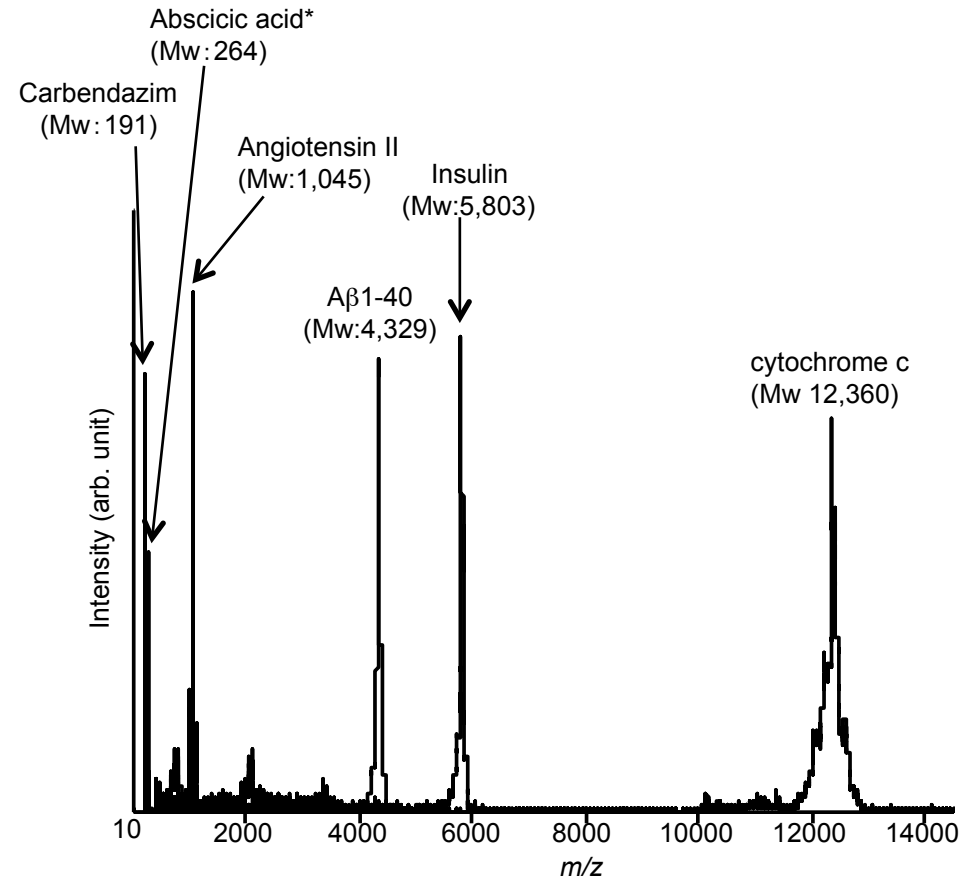


Figure 4 Nano-PALDI MS spectra of proteins, peptides, plant hormone and pesticide